Supporting Information Available:

Experiment Section

Preparation of **1**. A mixture of $CdCl_2 \cdot 2H_2O$ (0.219 g; 0.5 mmol), NaN_3 (0.032 g; 0.5 mmol), pyridine-4-sulfonic acid (0.080 g; 0.5 mmol) CH_3CN (3 mL) and H_2O (7 mL) was sealed in a 20 mL Teflonlined reactor, which was heated in an oven to 150 °C for 50 h, then cooled to room temperature at a rate of 5°C h^{-1}. Colorless block crystals were obtained in 65% yield, based on Cd. Elemental analysis (%) calcd for **1** ($C_6H_9Cd_3Cl_3N_{12}$), C, 10.40; H, 1.31; N, 24.26. Found: C, 10.43; H, 1.34, N, 24.24. Main IR frequencies (KBr, cm^{-1}): 3450, 2923, 1630, 1493, 1371, 1263, 1161, 1055, 694. **Warning: sodium azide is potentially explosive under the hydrothermal reaction conditions.** All crystallographic measurements were made on a Bruker SMART APEX II CCD area detector with graphite-monochromated Mo Ka radiation (λ = 0.71073 Å) operated at 2000 W power (50 kV, 30 mA). The structure was solved by direct methods and subsequent difference Fourier syntheses using the SHELXTL software suite. All non-hydrogen atoms were refined anisotropically. Crystallographic data for **1**: tetragonal $I\bar{4}2m$, with a = 22.2338(1) Å, c = 18.6223(2) Å, V = 9205.78(11) $Å^3$, Z = 16, μ(Mo Ka) = 3.108 mm^{-1}, ρ = 1.999 g cm^{-3}, T = 296 K, reflection numbers collected = 48756, unique reflections (R_{int}) = 4955 (0.0539), R_1 [I>2\s(I)] = 0.0319 and wR_2 (all data) = 0.0743, GOF = 1.055. CCDC 721872.

All tested photoluminescence of **1** interacting with other salts was investigated in the

solid state at room temperature. Compound **1** introduced as a powder (as prepared, 5 mg) into DMF solutions (2.00 mL) of different salts ($LiClO_4$, NH_4NO_3, $NaNO_3$, $Mg(NO_3)_2$, $Ba(NO_3)_2$, KI, LiCl, $NaNO_3$ and $NaNO_2$ at various concentrations ($1x10^{-4}$~$4x10^{-4}$ $molL^{-1}$). Ion-interacted products were isolated by filtration and drying at 50 °C for 24 h.

All materials and reagents were obtained commercially and used without further purification. Elemental (C, H, N) analyses were performed on a Perkin–Elmer 2400 elemental analyzer. Infrared (IR) samples were prepared as KBr pellets, and spectra were obtained in the 400~4000cm^{-1} range using a Nicolet Avatar 360 FT-IR spectrophotometer. The fluorescence spectra were measured using a Perkin-Elmer LS-55 spectrofluorimeter equipped with a pulsed xenon lamp as light source. Powder XRD investigations were carried out on a Bruker AXS D8-Advanced diffractometer at 40 kV, 40 mA with Cu Kα (λ =1.5406 Å) radiation at a scanning speed of 0.025°/sec over the 2θ range of 5–50°. XPS spectra were measured on a Perkin-Elmer model PHI 5600 XPS system with a resolution of 0.3–0.5 eV from a monochromated aluminium anode X-ray source. Time-of-Flight Secondary Ion Mass Spectrometry (ToF-SIMS) was carried out on a Physical Electronics PHI 7200 TOF-SIMS spectrometer. TGA experiments were performed on a NETZSCH TG 209 instrument with a heating rate of 10°C min^{-1} under N_2 atmosphere. Adsorption isotherms at 77 K were measured using an ASAP 2020 apparatus.

Explanations of the non-hydration and hydration compounds.

For the original dataset before hydration the largest 9 residual electron density peaks in the voids are the following:

Q1	1	0.000000	0.359200	0.000000	10.500000	0.050000	0.82
Q2	1	0.181800	0.181800	0.201300	10.500000	0.050000	0.68
Q5	1	0.018700	0.433600	0.017900	11.000000	0.050000	0.60
Q10	1	0.000000	0.406000	0.000000	10.500000	0.050000	0.54
Q13	1	0.405000	0.405000	0.200700	10.500000	0.050000	0.53
Q16	1	0.543600	0.543600	0.301100	10.500000	0.050000	0.51
Q17	1	0.070600	0.482300	0.016700	11.000000	0.050000	0.51
Q18	1	-0.019900	0.465300	0.016000	11.000000	0.050000	0.50
Q19	1	0.500000	0.500000	0.500000	10.125000	0.050000	0.50

These electron density peaks are within the normal background fluctuation as can be seen by the fact that many of the larger peaks are located not in the voids but close to the atoms of the framework (e.g. Q3, Q4, Q6, Q7, Q8, Q9, etc). They are also all below one electron per cubic Ångstrom.

After hydration all major residual electron density peaks are now located in the voids:

Q1	1	0.177800	0.177800	0.701400	10.500000	0.050000	1.87
Q2	1	0.156300	0.156300	0.688500	10.500000	0.050000	1.63
Q3	1	0.109000	0.109000	0.355000	10.500000	0.050000	1.25
Q4	1	0.000000	0.351300	0.500000	10.500000	0.050000	1.16
Q5	1	0.092300	0.092300	0.347800	10.500000	0.050000	1.08
Q6	1	0.401500	0.401600	0.140800	10.500000	0.050000	1.02
Q7	1	0.000000	0.042100	0.500000	10.500000	0.050000	0.89
Q8	1	0.083100	0.143900	0.645400	11.000000	0.050000	0.88
Q9	1	0.024400	0.500000	0.000000	10.500000	0.050000	0.72

They are larger in magnitude (up to nearly 2 electron per cubic Ångstrom). They are, however, still quite small which points towards significant disorder of any possible solvent molecules. Attempts were made to refine the residual electron density as disordered water molecules. This did not yield a satisfactory or unambiguous result. R values did drop, but not drastically. ADPs were very large and asymmetric, and no obvious solvate model was obvious (i.e. distances between water molecules and the atoms of the framework did not agree with expectations based on hydrogen bonding considerations).

Assuming disordered ill defined solavte molecules the electron density was instead corrected for using the Squeeze procedure implemented in the Program Platon (Version 40-M, A. L. Spek, 2009). It resulted in 6 solvate accessible voids: 4 small

voids with 169 or less cubic Ångstrom and 20 or less electrons per void and two major voids with 1134 cubic Ångstrom and 343 electrons per void (See complete list below). This indicated the presence of about 34 water molecules per void of 1134 cubic Ångstrom, or one water molecule per 33 cubic Ångstrom. This compares well with the volume of one molecule of water in bulk water (30 cubic Ångstrom International Tables of Crystallography Volume F) or the value used in the IUCR checkcif procedure (40 cubic Ångstrom)

```
loop_
   _platon_squeeze_void_nr
   _platon_squeeze_void_average_x
   _platon_squeeze_void_average_y
   _platon_squeeze_void_average_z
   _platon_squeeze_void_volume
   _platon_squeeze_void_count_electrons
    1   0.000   0.000   0.000       29        4
    2   0.000   0.500   0.000      169       20
    3   0.500   0.500   0.000     1137      343
    4   0.500   0.000   0.000      167       20
    5   0.000   0.000   0.500     1131      343
    6   0.000   0.500   0.500      167       20
    7   0.500   0.000   0.500      167       20
    8   0.500   0.500   0.500       21        3
_platon_squeeze_details
;
;
```

An equivalent analysis of the original dataset gave the following results:

```
loop_
   _platon_squeeze_void_nr
   _platon_squeeze_void_average_x
   _platon_squeeze_void_average_y
   _platon_squeeze_void_average_z
   _platon_squeeze_void_volume
   _platon_squeeze_void_count_electrons
    1   0.000   0.000   0.000     1154      114
    2   0.000   0.500   0.000      168       29
    3   0.500   0.000   0.000      168       29
    4   0.500   0.500   0.000       28        3
    5   0.500   0.500   0.500     1147      113
    6   0.000   0.500   0.500      168       29
    7   0.500   0.000   0.500      168       29
    8   0.000   0.000   0.500       21        2
```

_platon_squeeze_details
;
;

The result indicates that especially the two large voids have only one 33% of the electron as in the hydrated sample. This indicates that the voids in the non hydrated sample are indeed only partially filled.

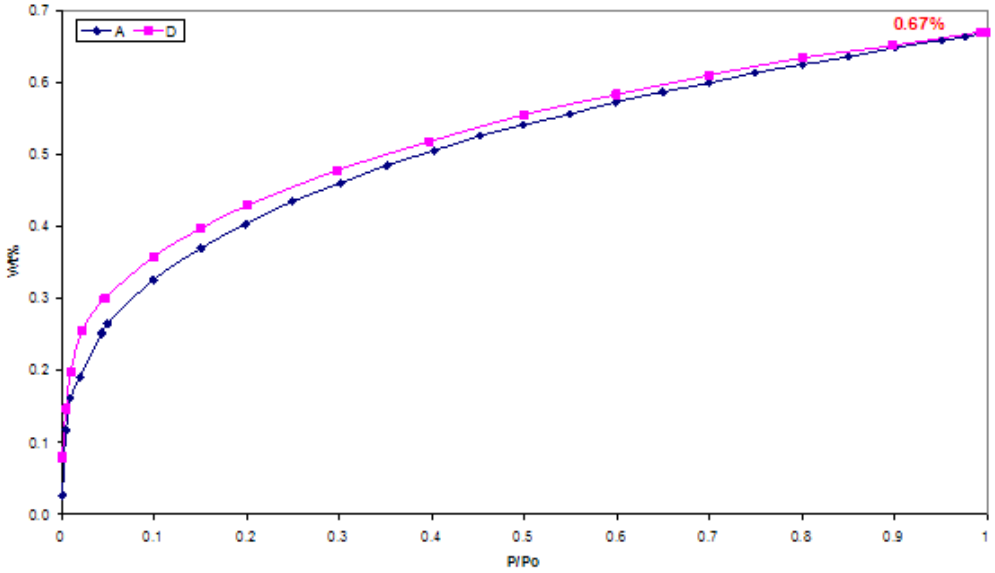

Figure S1. Diagram of H_2 adsorption isotherm of **1** at 77 K

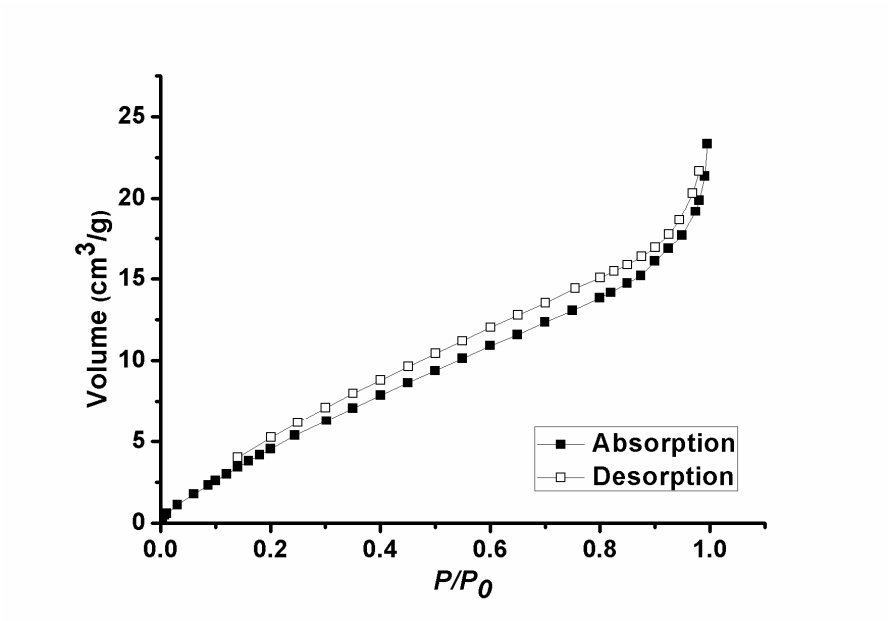

Figure S2. Diagram of N_2 adsorption isotherm of **1** at 77 K

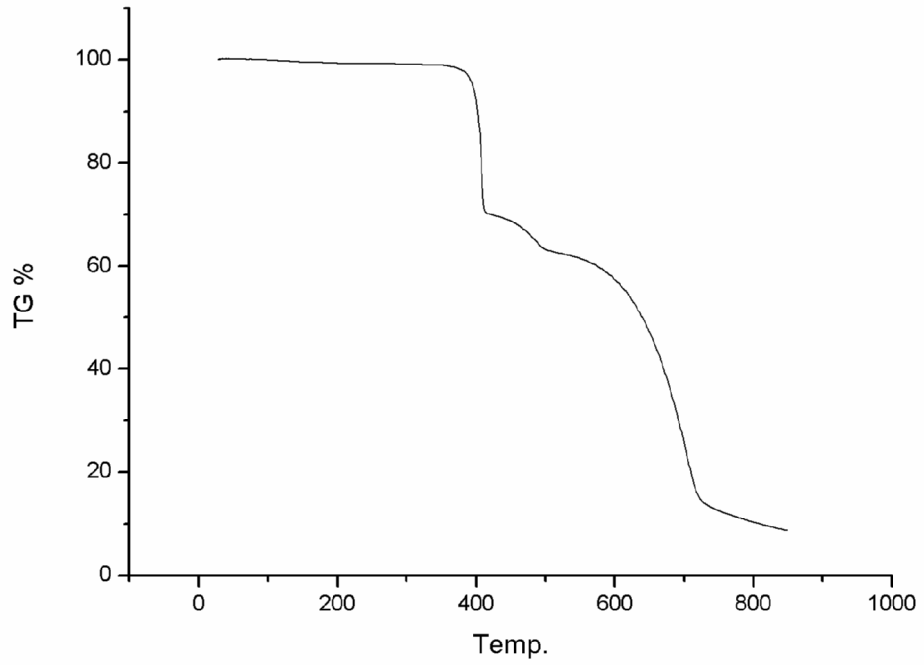

Figure S3. TGA trace of **1**.

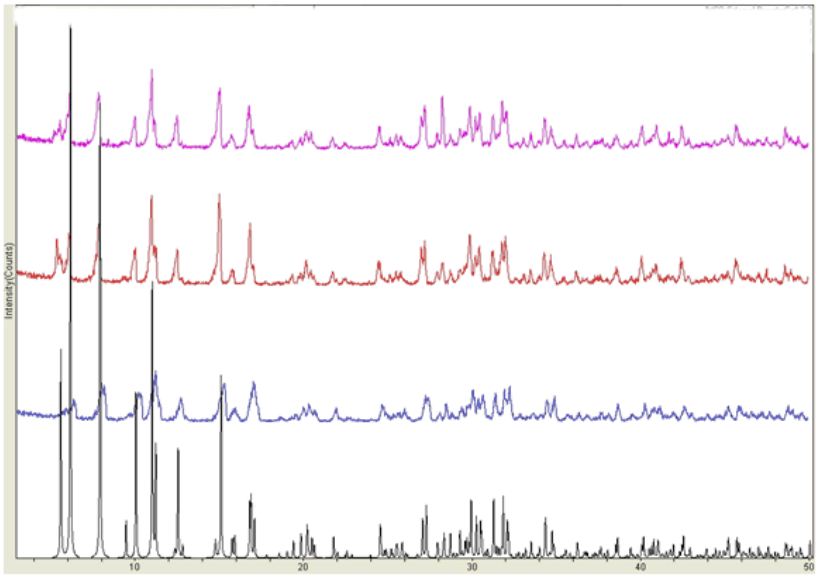

Figure S4. Powder xrd: Patterns of Simulated (black), as-prepared (blue), after outgassing (red) and after isotherm (pink)

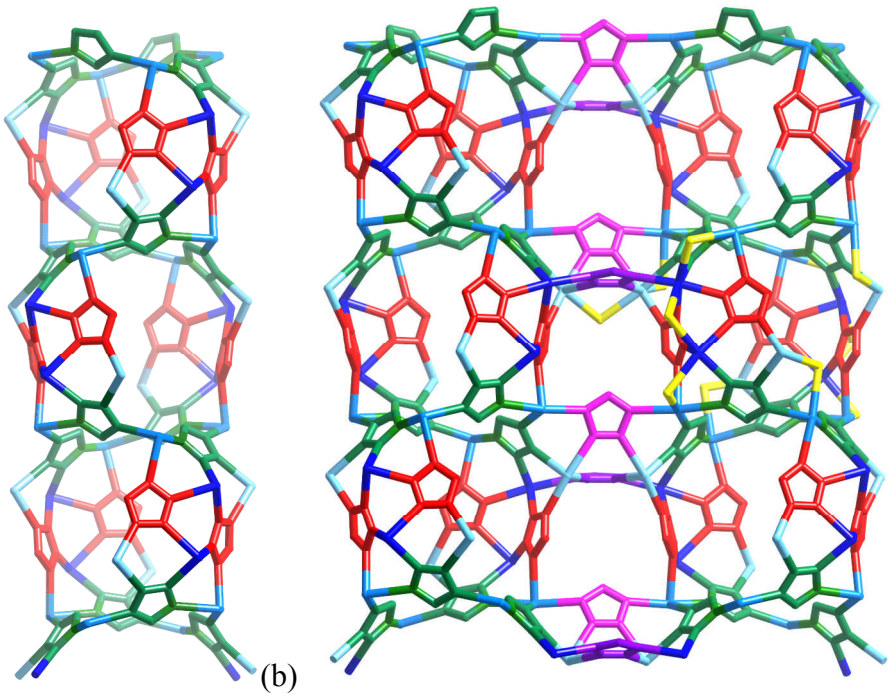

Figure S5. View of (a) a single Cd/5MT column in the structure of **1**, and (b) the joining of two adjacent columns by further 5MT ligands. For clarity, Cl bridges are only shown in part (b), and only for part of one column and for one bridge between columns. The colours for the ligands and metals are the same as for Figure 1.

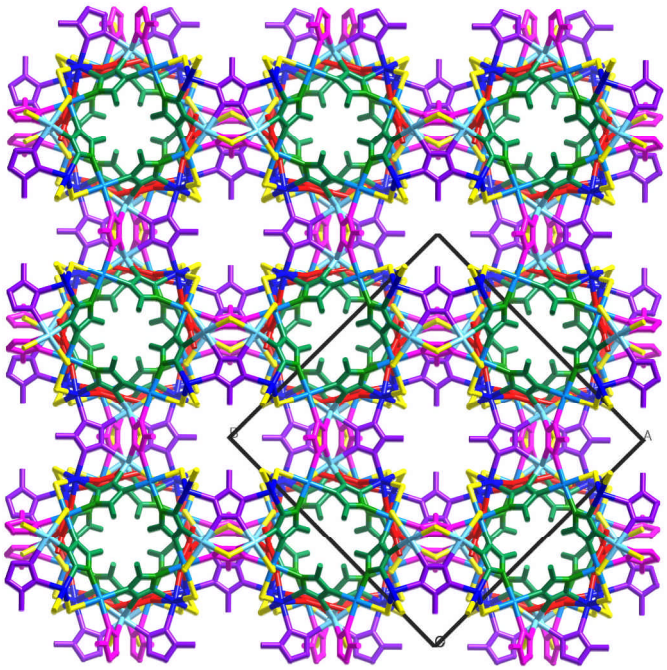

Figure S6. View of the overall connectivity of the structure, viewed end-on to the columns shown in Figure S5 (i.e. down the c-axis). Note each column (containing green and red 5MT ligands) is connected to six neighbouring columns via the pink and purple 5MT ligands. The view is analogous to Figure 1b, except chloride bridges and methyl groups have not been omitted.

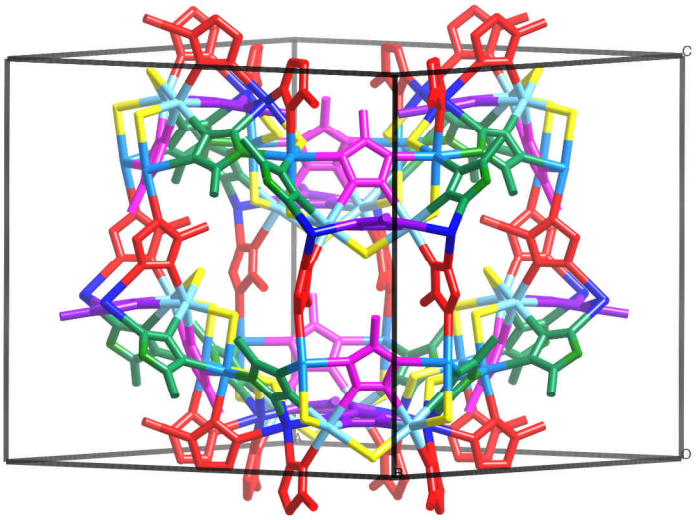

Figure S7. View of the largest cavity in the structure of **1**, which occupies a significant portion of the unit cell. The columns of Figure S5 run vertical in this viewpoint and lie in the vertical faces of the unit cell.

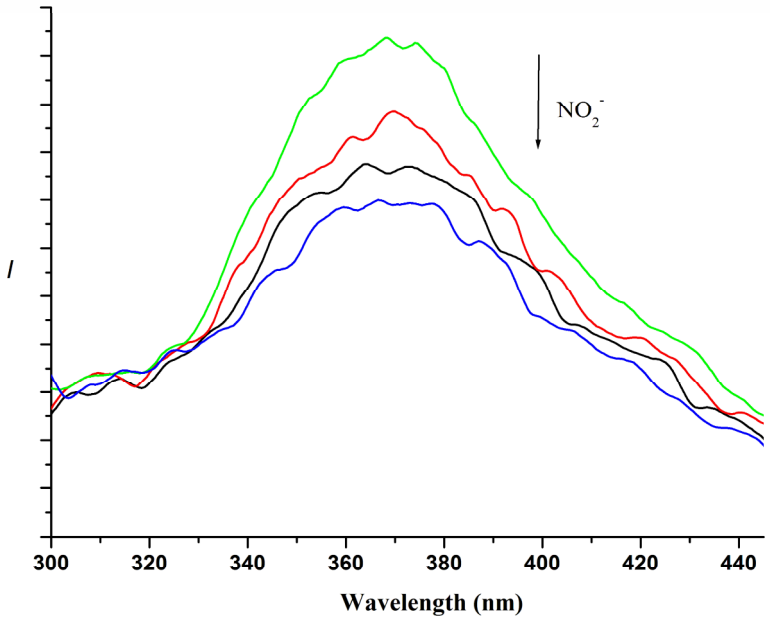

Figure S8. PL spectra of re-generated **1b** solids interacted in 0-3x10^{-4} mol L^{-1} $NaNO_2$ DMF solution.

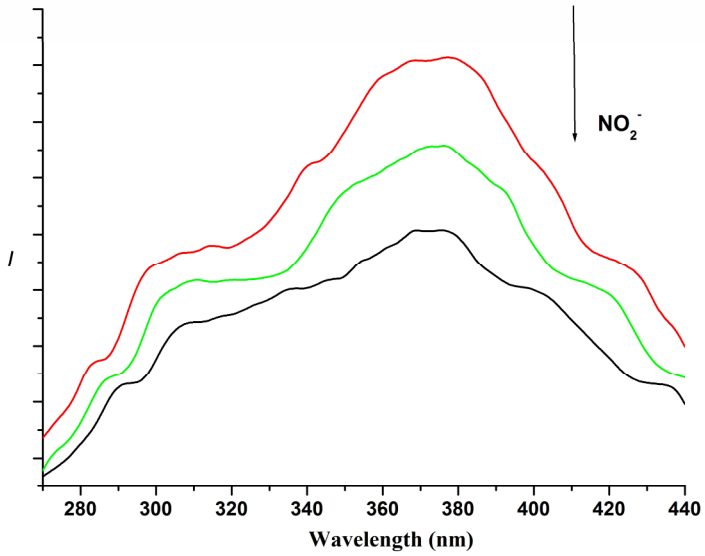

Figure S9. PL spectra of **1** solids interacted in 0-2 x10^{-4} mol L^{-1} $NaNO_2$ water solution.

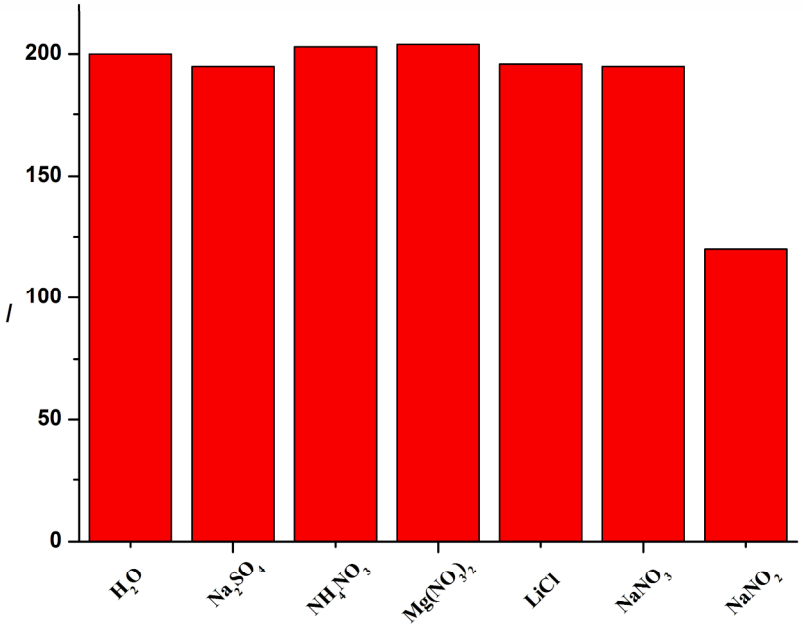

Figure S10. Comparison of the luminescence intensity of **1** interacting with different ions, de-activated in 1×10^{-4} molL^{-1} water solutions of different salts.

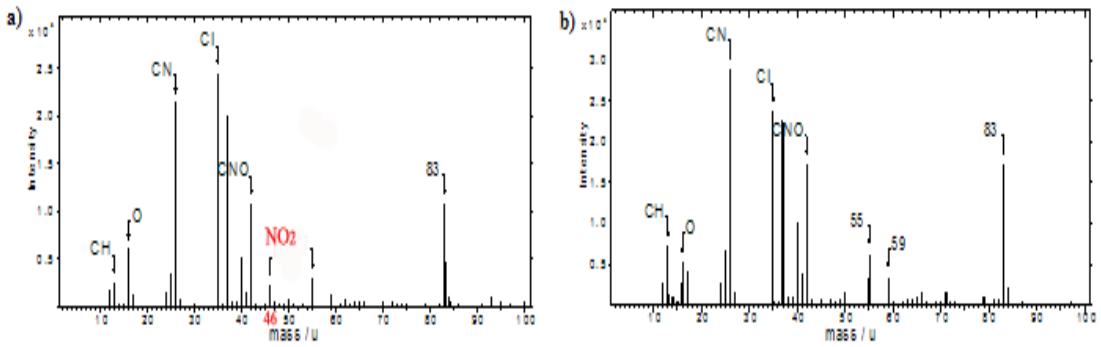

Figure S11. Time-of-Flight Secondary Ion Mass Spectrometry: a) nitrites interacted with solids **1** in $4x10^{-4}$ M DMF solution of $NaNO_2$, b) as-prepared **1**.

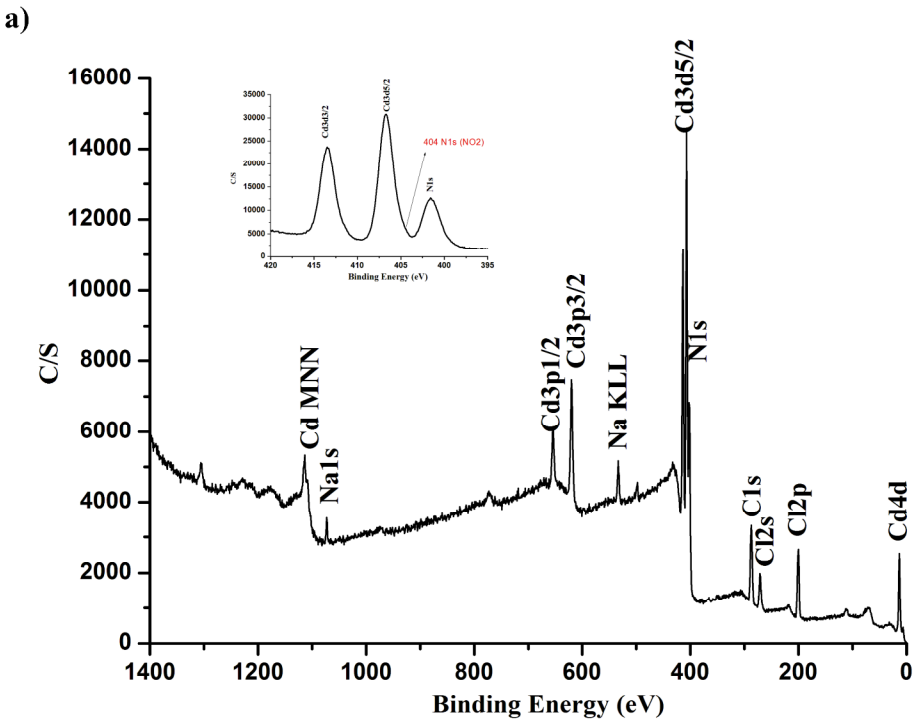

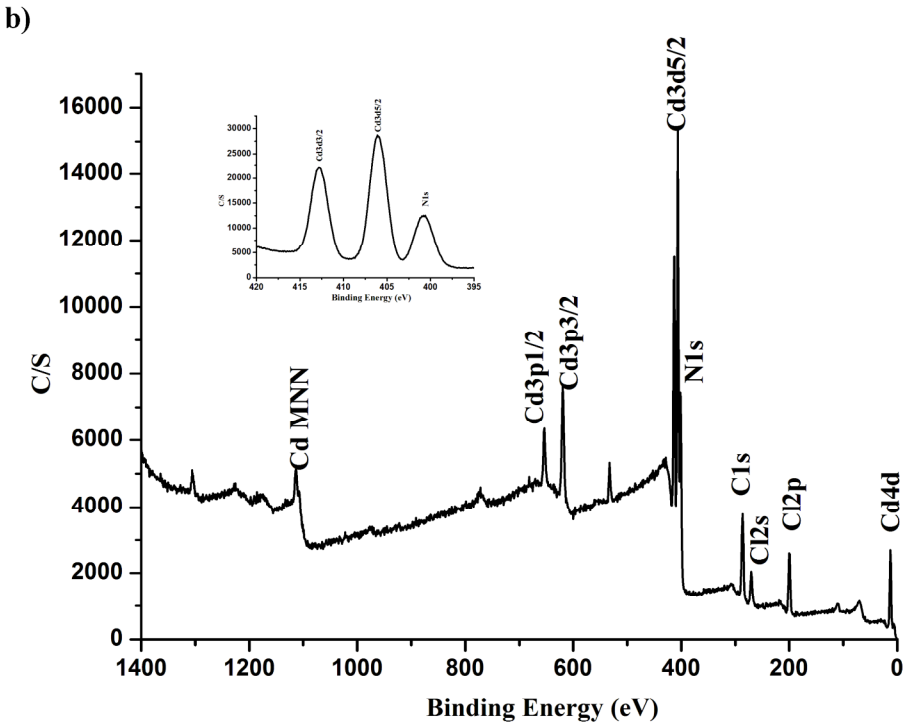

Figure S12. XPS Spectra: a) nitrites interacted with solids **1** in $4x10^{-4}$ M DMF solution of $NaNO_2$, b) the as-prepared **1**. [404 N1s peak (NO_2^-) overlaps with the peak (Cd3d5/2)].